Reports

Transition Between Frictional Slip and Ductile Flow for Halite Shear Zones at Room Temperature

TOSHIHIKO SHIMAMOTO*

A complete transition from frictional slip to ductile shearing flow upon decreasing velocity (or slip rate) or increasing confining pressure is documented for a thin layer of halite undergoing large shearing deformation. The results indicate that the logarithmic law for steady-state friction with a negative velocity dependence breaks down when friction becomes nearly equal to the shear resistance required for ductile flow and that the law changes into a flow law in shear upon further decrease in velocity. The friction-velocity relation is crucial in stability analyses of fault motion, and the results are important for earthquake and state-of-stress problems, especially in the application of laboratory data to the slow average motion of natural faults and to the behavior of deep faults along which ductile deformation becomes increasingly predominant.

ONE CHARACTERISTIC OF THE FRICtional properties of rocks is that, under many circumstances, steady-state friction is inversely proportional to the logarithm of the velocity along a fault (*1–7*). This logarithmic law with a negative velocity dependence is opposite in trend to the well-known strain-rate dependences of ductile flow and brittle failure of intact specimens in that both flow stress and failure stress increase with increasing strain rate (*8, 9*). The velocity dependence of steady-state friction is of fundamental importance in the framework of fault constitutive laws (*5–7*) and in the stability analysis of fault motion based thereon (*10–12*). In particular, it has been predicted that unstable motion or seismic slip of faults would be closely associated with the negative velocity dependence (*10*). Moreover, the crustal stress seems to be limited by the frictional strength of rocks (*13*), and hence the velocity dependence of friction is also important with respect to the problem of the state of stress, especially in the extrapolation of laboratory friction data to slow natural deformation.

Recent progress in the studies of fault constitutive properties is indeed remarkable, and it is now becoming possible to predict slip behavior of simulated faults and even earthquake phenomena based on friction laws established in laboratory friction experiments (*5–7, 10–12*). However, virtually all friction laws have been developed more or less empirically, and the physical bases for their extrapolation to long times and high temperatures are still poorly established. Empirical approaches are inevitable at this time, owing to the complexity of frictional processes, but at the same time their limitations are obvious. In an example reported recently (*14*), two empirical laws fitted laboratory friction data equally well and yet they predicted entirely different results when extrapolated to slow natural deformation.

In view of the present situation, several critical questions arise. (i) Is the logarithmic relation between friction and velocity valid at geological slip rates or at high temperatures and pressures? If not, under what conditions does it break down, or what is the criterion for the breakdown of the law? (ii) What is an alternative law when the logarithmic law is not valid? In this report I present a clue on how to answer these questions, although the approaches taken are still empirical.

Using a triaxial apparatus (*15*), I performed experiments at room temperature on dry, cylindrical specimens of Tennessee sandstone with a 0.3-mm-thick layer of halite along a precut surface at an angle of 35° to the cylindrical axis with slip rates along the precut surface ranging from 300 to 0.003 μm/sec (≃ 10 cm/year) and at confining pressures to 250 megapascals (MPa). Plastic deformation (in most cases accompanied by recrystallization) of halite in shear becomes noticeable at confining pressures above 35 MPa and becomes the most predominant deformation mechanism above 50 MPa at room temperature (*16*). Halite thus deforms by a wide spectrum of deformation mechanisms even at room temperature and is ideal for studying frictional properties in

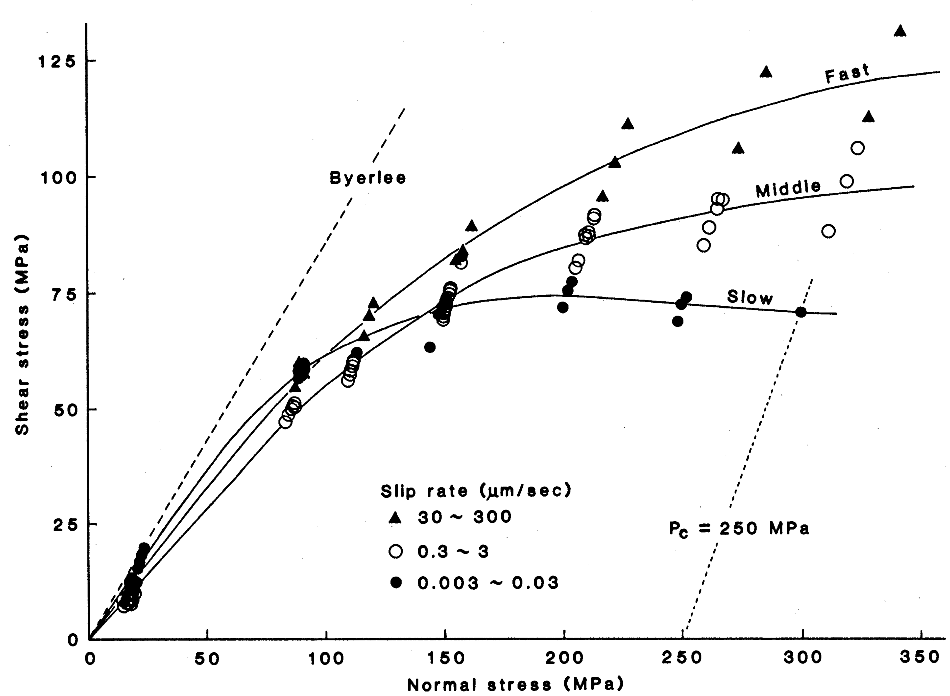

Fig. 1. Shear stress versus normal stress on the simulated fault at steady-state or nearly steady-state sliding for specimens of Tennessee sandstone with a 0.3-mm-thick, dry layer of synthetic halite (precompacted with a confining-pressure reduction experiment). Data are arranged in three groups for different ranges of slip rate along the precut suface. When stick-slip occurs, a regular stick-slip portion is selected and the stresses at the initiation of abrupt slip are plotted. The intersecting point of a straight line through each group of data with the abscissa gives the confining pressure for a test (for example, a run at 250 MPa). The dashed line indicates the frictional strength for many rocks (*21*).

Center for Tectonophysics, Texas A&M University, College Station 77843.

*Present address: Institute of Geology and Mineralogy, Faculty of Science, Hiroshima University, Hiroshima 730, Japan.

brittle, semibrittle, and ductile regimes. Halite is a useful analog of geologically important silicates for which precise measurements of frictional properties in all of these regimes cannot be made with currently available apparatuses.

Reagent-grade NaCl (about 0.1 mm in grain size) and cooking salt (natural halite of unknown origin, 0.2 to 0.3 mm in grain size) were used as the halite layers, whose thickness was estimated from weight (assuming zero porosity). Specimens deformed at confining pressures at and below 200 MPa were 4.8 cm in diameter and 9 to 11 cm long and those deformed at above 200 MPa were 3.8 cm in diameter and 6 to 7 cm long. Polyolefin shrink-fit tubes 3 mm thick were used as jackets. Stresses and specimen shortening were corrected for apparatus distortion, reduction in the apparent area of contact across the slip surfaces with displacement, and jacket strength (*17, 18*).

Because the velocity dependence of friction tends to be positive (that is, higher friction at faster slip rate) initially and becomes negative only after a certain displacement (*6*), some care is required in the design of experiments. In these tests I used a treatment for reducing the confining pressure that has been found effective in reducing this initial transient portion (*14, 19*). The slip rate along the simulated fault was changed either abruptly or after several minutes of halt in the shortening [see figure 1 in (*14*), figure 3 in (*19*), and figure 7 in (*20*)]. The slip rate was changed only after friction approached a steady-state value at the rate or after a regular stick-slip was attained.

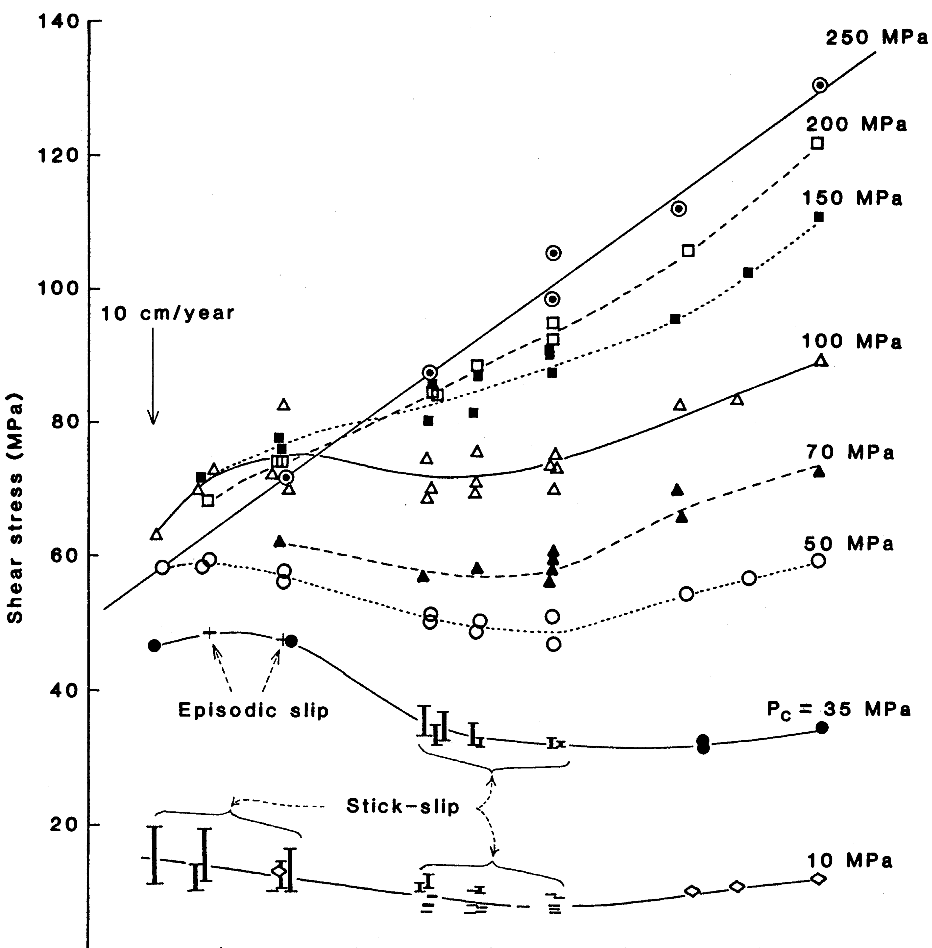

Fig. 2. Steady-state or nearly steady-state shear resistance (the shear stress on the precut surface) of a 0.3-mm-thick, dry layer of synthetic halite plotted against the common logarithm of slip rate along the precut surface. The results from eight runs at confining pressures as specified on the curves are plotted. When stick-slip occurs, a regular stick-slip portion is selected and the shear stresses at the onset and at the stop of abrupt slip events are tied with a thick vertical bar. The steady-state friction should fall between these stresses [see figures 3 through 6 in (*25*)]. The thickness of the horizontal line for episodic slip likewise indicates the range of shear-stress fluctuation. The run at a confining pressure of 35 MPa is the second run that was performed on the specimen deformed at 70 MPa after the displacement had been reset. All other runs in this figure and in Figs. 3 and 4 are on initially undeformed specimens.

Steady-state friction was not attained within an allowable displacement in some cases, especially at fast slip rates, in which the slip rate was changed even before the steady state was reached to determine nearly steady-state friction.

Figure 1 shows the shear stress and normal stress on the precut surface during steady-state or nearly steady-state frictional slip from seven runs on synthetic halite (0.3 mm thick) deformed at confining pressures to 250 MPa. The shear stress that can be sustained by the halite is slightly smaller than that for many rocks (*21*) at confining pressures below ~50 MPa, but the data deviate markedly from this at higher pressures (Fig. 1). The shear resistance of halite tends to become nearly independent of the normal stress at confining pressures above ~250 Mpa at fast slip rates, above 150 to 200 MPa at intermediate slip rates, and above ~100 MPa at slow slip rates. Moreover, the shear resistance is lowest at slow slip rates at pressures above ~100 Mpa, whereas it is lowest at the intermediate slip rates at pressures below ~90 MPa. Results similar to those in Fig. 1 were obtained for natural halite as well (*22*).

The shear resistance, τ, increases linearly with an increase in the logarithm of slip rate $\dot{\delta}$, at a confining pressure of 250 MPa, and the relation between τ and $\dot{\delta}$, can be expressed as (Figs. 2 and 3)

$$\tau = \tau_0 + p \log (\dot{\delta}/V_0) \qquad (1)$$

where p is a constant and τ_0 is the steady-state friction at a reference slip rate, V_0. Least-squares fit to the data in Figs. 2 and 3 yields $p = 13$ Mpa, $\tau_0 = 96$ MPa, and $V_0 = 1$ μm/sec. If we assume homogeneous simple shear of halite, a good fit to the same data is obtained by use of a power law of the form (Fig. 4)

$$\dot{\gamma} = q\tau^n \qquad (2)$$

where $\dot{\gamma}$ is the shear-strain rate, and q and n are constants ($q = 5.56 \times 10^{-37}$ MPa^{-n} sec^{-1} and $n = 17.3$ for the data in Fig. 4). It is unclear at this time which of these equations is valid over wider slip rates. Equation 2 has the same form as the well-known power law for the steady-state flow of rocks and minerals, although the stress exponent, n, for halite in shear is about three times the value for pure-shear deformation of cylindrical specimens (*23*). Perhaps halite is completely in the pressure-insensitive flow regime at a pressure of 250 MPa.

A regime of negative velocity dependence of friction is present at confining pressures below about 100 MPa (Figs. 2 and 3), and it will be called here "frictional regime" (Fig. 5). Stick-slip was recognized only in this regime, consistent with a theoretical predic-

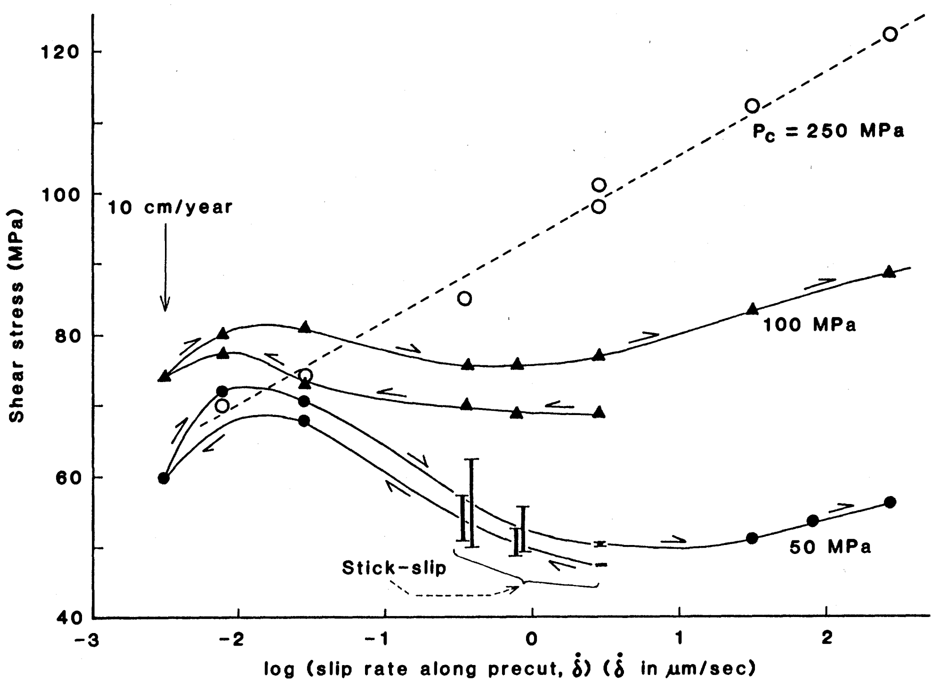

Fig. 3. Steady-state or nearly steady-state shear resistance of a 0.3-mm-thick, dry layer of natural halite plotted against the common logarithm of slip rate along the precut surface. Arrows point toward a later stage of each run.

tion (*10*). The negative velocity dependence of friction changes into a positive dependence upon a reduction in the slip rate when the friction becomes nearly equal to the shear resistance in the pressure-insensitive flow regime at a pressure of 250 MPa (Figs. 2 and 3). Evidently, this turning point was not reached in a run at 10 MPa, and stick-slip occurred even at the slowest slip rates (Fig. 2). The velocity dependence becomes positive at fast slip rates (Figs 2 and 3; high-speed frictional regime in Fig. 5). Presumably because of this barrier against slip acceleration at high slip rates, abrupt slip events of halite were much slower phenomena than those during bare-rock frictional sliding of sandstone for which Dieterich observed a nearly constant friction at fast slip rates (*3*). With increasing confining pressure, the regime of negative velocity dependence shrinks down, the slope of the friction-velocity curve in the high-speed frictional regime increases, and eventually the friction-velocity curve degenerates into the curve for the pressure-insensitive ductile flow (Figs. 2 and 3).

If these results for halite are general, the two questions posed earlier can be answered as follows. (i) As the velocity, $\dot{\delta}$, is reduced, the logarithmic law with a negative velocity dependence breaks down when friction becomes nearly equal to the shear resistance required for ductile flow. (ii) The law changes into a flow law upon further reduction in $\dot{\delta}$ (Fig. 5). For fault motion at depth, the flow and friction laws at appropriate temperature and pressure must be used. The critical velocity, $\dot{\delta}_{cr}$, at which the logarithmic law breaks down is probably too slow to be determined by laboratory experiments for many brittle rocks and minerals. But the above criterion would enable one to estimate the critical velocity by extrapolating the flow law and the friction law, both determined in short-term experiments, toward the slower velocity and by taking their intersecting point (Fig. 5). Thus the criterion is of potential importance in applying laboratory data to earthquake and state-of-stress problems at deeper levels where ductile behavior becomes increasingly important.

Detailed observations of deformed halite have revealed that the flow regime and frictional regime in Fig. 5 correspond to the

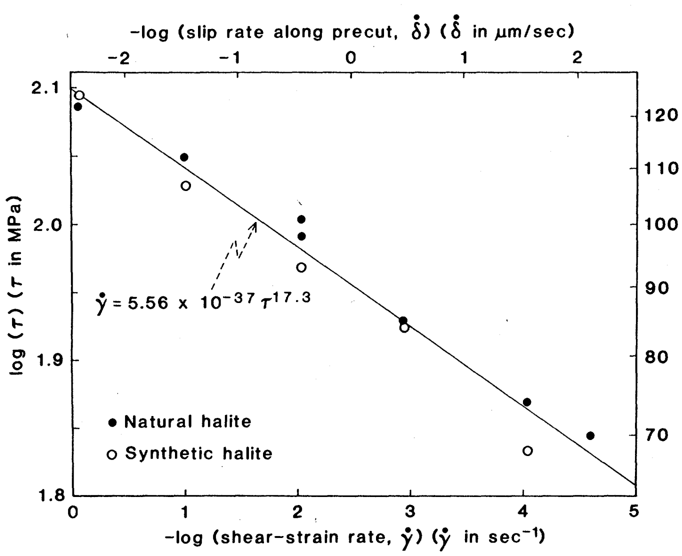

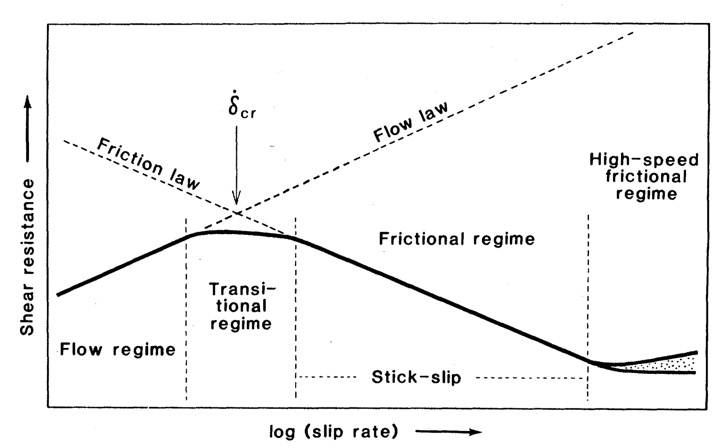

Fig. 4 (left). Steady-state or nearly steady-state shear resistance of a 0.3-mm-thick dry layer of halite plotted against the average shear-strain rate within halite shear zones at a confining pressure of 250 MPa (pressure-insensitive flow regime at room temperature). The strain rate is estimated from the slip rate along the precut surface and the thickness of shear zones (homogeneous simple-shear deformation is assumed). The solid line is the least-squares fit to the data. Fig. 5 (right). A schematic diagram showing the transition from frictional slip to ductile flow at slow slip rates. Friction is lower than the expected flow stress at fast and intermediate slip rates, and vice versa at slow slip rates. Stick-slip occurs only in the frictional regime with a negative velocity dependence of friction (that is, lower friction at a faster slip rate). The velocity dependence of friction in the high-speed frictional regime greatly affects the dynamic motion of a fault during stick-slip. The velocity, $\dot{\delta}_{cr}$, at the intersecting point of the flow law and the friction law gives the approximate critical velocity at which the logarithmic friction law breaks down.

homogeneous shearing deformation and to the heterogeneous and localized deformation of halite layer, respectively (*22*). The detailed analysis of this heterogeneous deformation is an important future task necessary for understanding the mechanism of seismogenic slip of a fault. The results in Figs. 1 through 3 are important with respect to the origin of large or great thrust-type earthquakes in subduction zones (*20*). Stability analyses of simulated fault are also needed to determine the fault constitutive laws in the brittle, semibrittle, and ductile regimes. These will provide rigorous information on necessary parameters in the modeling of fault motion at seismogenic depths and at deeper levels along plate boundaries. Existing fault constitutive laws (*5–7*) will need to be modified and extended to describe the fault motion in all of the deformation regimes [see also (*24*)].

The results in Figs. 2 and 3 have important implications concerning the long-term behavior of faults. Because all friction laws have been established empirically on the basis of short-term laboratory tests, there is no guarantee that they hold for slow natural deformation. However, halite data at slow rates (down to 10 cm/year) are encouraging since no peculiar long-term behavior has been observed. For instance, the logarithmic law with negative velocity dependency holds almost until the behavior changes into ductile shearing flow with decreasing velocity (Fig. 5). Perhaps most friciton laws are applicable to the slow motion of natural faults.

REFERENCES AND NOTES

1. J. H. Dieterich, *Trans. Am. Geophys. Union* **56**, 1959 (1975).
2. C. H. Scholz and J. T. Engelder, *Int. J. Rock Mech. Min. Sci. Geomech. Abstr.* **13**, 149 (1976).
3. J. H. Dieterich, *Pure Appl. Geophys.* **116**, 790 (1978).
4. L. W. Teufel and J. M. Logan, *ibid.*, p. 840.
5. J. H. Dieterich, *J. Geophys. Res.* **84**, 2161 (1979).
6. ——, *Geophys. Monogr. Am. Geophys. Union* **24**, 103 (1981).
7. A. L. Ruina, *J. Geophys. Res.* **88**, 10359 (1983).
8. A. Nicolas and J. P. Poirier, *Crystalline Plasticity and Solid State Flow in Metamorphic Rocks* (Wiley, New York, 1976).
9. M. S. Paterson, *Experimental Rock Deformation: The Brittle Field* (Springer, New York, 1978).
10. J. R. Rice and A. L. Ruina, *J. Appl. Mech.* **50**, 343 (1983).
11. J. R. Rice and J.-c. Gu, *Pure Appl. Geophys.* **121**, 187 (1983).
12. J.-c. Gu, J. R. Rice, A. L. Ruina, S. T. Tse, *J. Mech. Phys. Solids* **32**, 167 (1984).
13. W. F. Brace and D. L. Kohlstedt, *J. Geophys. Res.* **85**, 6248 (1980).
14. T. Shimamoto and J. M. Logan, *Tectonophysics* **109**, 165 (1984).
15. J. W. Handin, M. Friedman, J. M. Logan, L. J. Pattison, H. S. Swolfs, *Geophys. Monogr. Am. Geophys. Union* **16**, 1 (1972); T. Shimamoto, J. W. Handin, J. M. Logan, *Tectonophysics* **67**, 175 (1980).
16. H. Hiraga and T. Shimamoto, unpublished data; S. T. Knapp, thesis, Texas A&M University (1983).
17. T. Shimamoto, thesis, Texas A&M University (1977).
18. —— and J. M. Logan, *J. Geophys. Res.* **86**, 2901 (1981).
19. T. Shimamoto, *Int. J. Rock Mech. Min. Sci. Geomech. Abstr.* **22**, 227 (1985).
20. ——, *Tectonophysics* **119**, 37 (1985).
21. J. D. Byerlee, *Pure Appl. Geophys.* **116**, 615 (1978).
22. T. Shimamoto and J. M. Logan, *ibid.*, in press.
23. H. C. Heard, *Geophys. Monogr. Am. Geophys. Union* **16**, 191 (1972).
24. J. D. Weeks and T. E. Tullis, *J. Geophys. Res.* **90**, 7821 (1985).
25. J. R. Rice and S. T. Tse, personal communication.

26. I thank J. M. Logan and J. H. Dietrich for their review of the manuscript. Supported under U.S. Geological Survey contracts 14-18-0001-19293 and 14-08-0001-21181.

26 August 1985; accepted 7 November 1985

Palynological and Iridium Anomalies at Cretaceous-Tertiary Boundary, South-Central Saskatchewan

D. J. Nichols, D. M. Jarzen, C. J. Orth, P. Q. Oliver

The Cretaceous-Tertiary boundary in south-central Saskatchewan is marked by coincident anomalies in abundance of iridium and fern spores at the extinction level of a suite of Cretaceous pollen taxa. Evidence of disruption of the terrestrial flora includes the fern-spore abundance anomaly and local extinction of as much as 30 percent of angiosperm species. The reorganized earliest Tertiary flora is made up largely of surviving species that assumed new roles of dominance. Persistence of climatically sensitive taxa across the boundary indicates that if paleoclimate was altered by the terminal Cretaceous event, it returned quickly to the pre-event condition.

Orth *et al.* (*1*) recorded the occurrence of an anomalous concentration of iridium at the palynologically defined Cretaceous-Tertiary (K/T) boundary in a nonmarine stratigraphic sequence. According to Alvarez *et al.* (*2*), the excess iridium is of extraterrestrial origin and was deposited as a result of a large bolide impact. An alternative proposal (*3*) is that the iridium is of deep terrestrial origin and was deposited as a consequence of volcanism. The occurrence of the geochemical anomaly coincides with land-plant extinctions that mark the K/T boundary in western North America (*4, 5*). Irrespective of its cause, studies of the terminal Cretaceous event (TCE) and its effects on the nonmarine realm, with particular reference to effects on plants, are important because they have implications for possible analogies between impact and nuclear winter scenarios (*6*). Studies in nonmarine rocks in western North America (*7–10*) revealed the presence of the iridium anomaly at the palynologically defined K/T boundary at numerous sites in New Mexico, Colorado, and Montana.

We found sharply defined palynological and iridium anomalies at the K/T boundary near Morgan Creek, south-central Saskatchewan, about 165 km north of previously known sites in Montana and 1200 km north of the original site in New Mexico. The K/T boundary at Morgan Creek is characterized by extinctions of pollen taxa and the anomalous abundance of fern spores that are further evidence of an abrupt, continent-wide disturbance of the terrestrial ecosystem at the end of Cretaceous time (*4*). A second fern-spore abundance anomaly of uncertain significance is present more than 3 m above the boundary. Palynological data are evidence of paleoclimates immediately preceding and following the TCE, and they document major changes leading to the development of the earliest Tertiary flora. Geochemical data from this site bear on postdepositional behavior of iridium at the K/T boundary.

The K/T boundary in southern Saskatchewan is approximately at the contact between bentonitic mudstones and siltstones of the Frenchman Formation (late Maestrichtian) and the overlying Ravenscrag Formation (early Paleocene), which consists of sandstones, siltstones, mudstones, carbonaceous shales, and coals. These units were deposited in alluvial, lacustrine, and paludal environments associated with final retreat of the Cretaceous epicontinental sea. The Frenchman and Ravenscrag formations are, respectively, the stratigraphic equivalents of the Hell Creek and Fort Union formations in Montana. In these sequences the K/T boundary approximates the lithologic boundary between coal-bearing strata and

D. J. Nichols, U.S. Geological Survey, Denver, CO 80225.
D. M. Jarzen, National Museums of Canada, Ottawa, Ontario KlA 0M8.
C. J. Orth and P. Q. Oliver, Los Alamos National Laboratory, Los Alamos, NM 87545.